



# Pressure separation—a technique for improving the velocity error in finite element discretisations of the Navier–Stokes equations

Sashikumaar Ganesan, Volker John \*

*Institut für Analysis und Numerik, Otto-von-Guericke-Universität Magdeburg, Postfach 4120, 39016 Magdeburg, Germany*

---

## Abstract

This paper presents a technique to improve the velocity error in finite element solutions of the steady state Navier–Stokes equations. This technique is called pressure separation. It relies upon subtracting the gradient of an appropriate approximation of the pressure on both sides of the Navier–Stokes equations. With this, the finite element error estimate can be improved in the case of higher Reynolds numbers. For practical reasons, the pressure separation can be applied above all for finite element discretisations of the Navier–Stokes equations with piecewise constant pressure. This paper presents a computational study of five ways to compute an appropriate approximation of the pressure. These ways are assessed on two- and three-dimensional examples. They are compared with respect to the error reduction in the discrete velocity and the computational overhead.

© 2004 Elsevier Inc. All rights reserved.

*Keywords:* Steady state Navier–Stokes equations; Finite element methods; Low order non-conforming discretisations; Pressure separation; Error reduction

---

\* Corresponding author.

*E-mail address:* [ga.sashikumaar@mathematik.uni-magdeburg.de](mailto:ga.sashikumaar@mathematik.uni-magdeburg.de) (S. Ganesan).

## 1. Introduction

The steady state motion of an incompressible fluid is governed by the steady state Navier–Stokes equations

$$\begin{aligned} -Re^{-1}\Delta\mathbf{u} + (\mathbf{u} \cdot \nabla)\mathbf{u} + \nabla p &= \mathbf{f} \quad \text{in } \Omega, \\ \nabla \cdot \mathbf{u} &= 0 \quad \text{in } \Omega, \\ \mathbf{u} &= \mathbf{g} \quad \text{on } \partial\Omega, \end{aligned} \tag{1}$$

where  $\Omega \subset \mathbb{R}^d$ ,  $d \in \{2, 3\}$ , is a bounded domain with Lipschitz boundary  $\partial\Omega$ . The Reynolds number  $Re > 0$ , the body forces  $\mathbf{f}$  and the boundary conditions  $\mathbf{g}$  are given.

Finite element methods are one of the most popular approaches to discretise (1). A lot of analytical results for finite element discretisation of (1) are available, see [4] for an overview. Recently, there have been investigations of techniques to improve the accuracy of finite element solutions of (1) beyond the standard analytical results. For example, in [14], superconvergence results on uniform grids are proven. If all the assumptions for the application of this technique are fulfilled, one can obtain with a reasonable additional overhead a considerable increase in the accuracy of the numerical solution.

This paper considers a technique to increase the accuracy of the computed velocity in the case of a higher Reynolds number, i.e. the Navier–Stokes equations (1) are convection-dominated, and of the pressure being large in a certain (semi-)norm. In this case, it turns out that one of the dominating terms in the finite element error estimate is the product of the Reynolds number and the norm of the pressure. The simple idea consists now to modify the Navier–Stokes equations (1) such that the norm of the pressure in the modified equations is much smaller than the norm of the original pressure. This approach is called pressure separation. The key idea of the pressure separation is to compute a so-called separated pressure  $p_{\text{sep}}$ , which is a good approximation on  $p$ , and to subtract the gradient of  $p_{\text{sep}}$  from both sides of the first equation in (1). It dates back already from the middle of the 90s, [3, 18]. A small number of two-dimensional numerical tests can be found in [18, 6].

This paper contains, to our knowledge, the first thorough numerical study of the pressure separation. Although the application of the pressure separation gives only an improvement in the constant in the velocity error estimate and not in the order of convergence, the numerical studies will show that the discrete velocity with pressure separation might be considerably more accurate than without. There is a lot of freedom for computing  $p_{\text{sep}}$ . We will study in this paper five different variants, see Section 3. The first two variants are based on an appropriate modification of discrete pressures which are computed by discretising the original Navier–Stokes equations (1). In the other three variants, appropriate auxiliary problems are solved to compute a function  $p_{\text{sep}}$ .

The numerical study will assess these five variants based on the accuracy of the results and the computational overhead.

In practical computations, the separated pressure  $p_{\text{sep}}$  will be a finite element function. Thus,  $p_{\text{sep}}$  possesses only a limited regularity,  $p_{\text{sep}} \in H^1(\Omega)$ , and it turns out that in this case the idea of pressure separation works if the Navier–Stokes equations are discretised using a piecewise constant pressure space, see Section 2. Appropriate velocity finite element spaces, which fulfill the inf–sup stability condition with a piecewise constant pressure space are, e.g., non-conforming spaces of first order [2,1,15,13]. Thus, we will restrict our numerical study to such pairs of finite element spaces. It is well known that the numerical results with these pairs of finite element spaces are quite inaccurate in comparison with higher order finite element spaces, [17,10,7]. However, they can be an important tool in the efficient solution of the discrete systems arising from higher order discretisations, see [10,7,9] for the so-called multiple discretisation multilevel method. In this multilevel method, lowest order non-conforming discretisation are used on all coarser levels of the multigrid hierarchy. The higher order discretisation is applied only on the finest level. This approach uses the well-known efficiency of multigrid methods for lowest order discretisations [20,12]. The numerical studies in [10,7] show that the multiple discretisation multilevel approach might work considerably more efficient than the standard multigrid approach. Improving the accuracy of finite element solutions for non-conforming finite element discretisations of lowest order will result in an increased efficiency of the multiple discretisation multilevel method. For this reason, the study of techniques which improve the accuracy of low order discretisations is of interest.

The paper is organised as follows. Section 2 presents the idea of pressure separation in detail. The five variants of computing a function  $p_{\text{sep}}$  are described in Section 3. Section 4 contains the numerical tests on two- and three-dimensional examples. A detailed evaluation of these tests can be found in Section 4.3. The results are summarised in Section 5.

## 2. The motivation of the pressure separation

Standard notations of Lebesgue and Sobolev spaces are used throughout this paper. The norm in  $(L^2(\Omega))^d$ ,  $d \in \{1, 2, 3\}$ , is denoted by  $\|\cdot\|_{L^2}$ , the norm in  $(H^k(\Omega))^d$  by  $\|\cdot\|_{H^k}$ ,  $k \geq 1$ , and the semi norm in  $(H^k(\Omega))^d$  by  $|\cdot|_{H^k}$ .

We consider the application of a Galerkin finite element method for the numerical solution of (1). Let  $(V^h, Q^h)$  be a pair of velocity–pressure finite element spaces fulfilling the inf–sup stability condition where the functions from  $V^h$  are piecewise polynomials of order  $k$ ,  $k \geq 1$ , and the functions from  $Q^h$  are piecewise polynomials of order  $k - 1$ , e.g., see [4,5] for the inf–sup condition and examples of appropriate spaces. We assume that (1) has a unique

solution  $(\mathbf{u}, p) \in (H^{k+1}(\Omega))^d \times H^k(\Omega)$ . This implies a smallness assumption on the data and on the Reynolds number, see [4, Chapter IV, Theorem 2.3] for details. Denote the finite element solution by  $(\mathbf{u}^h, p^h)$  and let  $h$  be the mesh width of an underlying quasi-uniform triangulation of  $\Omega$ .

The idea of the pressure separation can be motivated in a very simple way on the Stokes equations with homogeneous Dirichlet boundary conditions

$$\begin{aligned} -\Delta \mathbf{u} + \nabla p_1 &= \mathbf{f} \quad \text{in } \Omega, \\ \nabla \cdot \mathbf{u} &= 0 \quad \text{in } \Omega, \\ \mathbf{u} &= \mathbf{0} \quad \text{on } \partial\Omega. \end{aligned} \tag{2}$$

With the assumptions on the finite element spaces from above, the finite element error estimate for (2) is, [4, Chapter II],

$$h|\mathbf{u} - \mathbf{u}^h|_{H^1} + \|\mathbf{u} - \mathbf{u}^h\|_{L^2} \leq Ch^{k+1}(|\mathbf{u}|_{H^{k+1}} + |p_1|_{H^k}), \tag{3}$$

where the constant  $C$  depends on  $\Omega$  and the solution of (2) is assumed to be sufficiently regular. We consider now the Stokes problem with weighted diffusive term

$$\begin{aligned} -Re^{-1}\Delta \mathbf{u} + \nabla p &= \mathbf{f} \quad \text{in } \Omega, \\ \nabla \cdot \mathbf{u} &= 0 \quad \text{in } \Omega, \\ \mathbf{u} &= \mathbf{0} \quad \text{on } \partial\Omega. \end{aligned} \tag{4}$$

This problem is equivalent to

$$\begin{aligned} -\Delta \mathbf{v} + \nabla p &= \mathbf{f} \quad \text{in } \Omega, \\ \nabla \cdot \mathbf{v} &= 0 \quad \text{in } \Omega, \\ \mathbf{v} &= \mathbf{0} \quad \text{on } \partial\Omega, \end{aligned} \tag{5}$$

with  $\mathbf{v} = Re^{-1}\mathbf{u}$ . Applying the error estimate (3) to the solution of (5) and transforming back to the solution of (4) give

$$h|\mathbf{u} - \mathbf{u}^h|_{H^1} + \|\mathbf{u} - \mathbf{u}^h\|_{L^2} \leq Ch^{k+1}(|\mathbf{u}|_{H^{k+1}} + Re|p|_{H^k}), \tag{6}$$

where  $C$  depends on  $\Omega$ . In the case that  $Re$  is high, the second term in the error estimate (6) possesses a large weighting factor. In addition, if  $|p|_{H^k(\Omega)}$  is large, the right hand side of the error estimate is dominated by the second term. For the Navier–Stokes equations (1), one can make a similar observation. If the Reynolds number  $Re$  is higher and if the  $H^k$ -semi norm of the pressure is large, then the product of these terms is a dominant term on the right hand side of the finite element error estimate. However, there might be also other terms on the right hand side of this estimate whose importance increases if the Reynolds number becomes higher, see [18, p. 87].

The goal of the pressure separation is to improve the right hand side of (6) for the situation that  $Re$  and  $|p|_{H^k(\Omega)}$  are large. Instead of (4), the following problem is considered:

$$\begin{aligned} -Re^{-1}\Delta\mathbf{u} + \nabla(p - p_{\text{sep}}) &= \mathbf{f} - \nabla p_{\text{sep}} \quad \text{in } \Omega, \\ \nabla \cdot \mathbf{u} &= 0 \quad \text{in } \Omega, \\ \mathbf{u} &= \mathbf{0} \quad \text{on } \partial\Omega. \end{aligned} \tag{7}$$

Here, the separated pressure  $p_{\text{sep}}$  is a known function such that  $|p - p_{\text{sep}}|_{H^k}$  is much smaller than  $|p|_{H^k}$ . Instead of (6), one obtains the error estimate

$$h|\mathbf{u} - \mathbf{u}_{\text{sep}}^h|_{H^1} + \|\mathbf{u} - \mathbf{u}_{\text{sep}}^h\|_{L^2} \leq Ch^{k+1}(|\mathbf{u}|_{H^{k+1}} + Re|p - p_{\text{sep}}|_{H^k}), \tag{8}$$

where  $\mathbf{u}_{\text{sep}}^h$  is the velocity solution of the Galerkin finite element approximation of (7).

For the Navier–Stokes equations, one can apply the same idea. That means, instead of (1), the pressure separated Navier–Stokes equations

$$\begin{aligned} -Re^{-1}\Delta\mathbf{u} + (\mathbf{u} \cdot \nabla)\mathbf{u} + \nabla(p - p_{\text{sep}}) &= \mathbf{f} - \nabla p_{\text{sep}} \quad \text{in } \Omega, \\ \nabla \cdot \mathbf{u} &= 0 \quad \text{in } \Omega, \\ \mathbf{u} &= \mathbf{g} \quad \text{on } \partial\Omega \end{aligned} \tag{9}$$

are solved. In this paper, we will study numerically the effect of solving (9) instead of (1) on the accuracy of the discrete velocity.

From the practical point of view,  $p_{\text{sep}}$  will be represented by a finite element function. Using a standard conforming finite element space for  $p_{\text{sep}}$ , then  $p_{\text{sep}} \in H^1(\Omega)$  but  $p_{\text{sep}} \notin H^2(\Omega)$ . That means, the last term in the error estimate (8) is well defined only for  $k = 1$ . The condition on the finite element spaces formulated above imply that the discrete velocity is of first order and the discrete pressure is piecewise constant ( $Q^h = P_0$  or  $Q^h = Q_0$ ). First order velocity spaces which fulfill the inf–sup condition with piecewise constant pressure spaces are on triangular grids the non-conforming Crouzeix–Raviart space  $V^h = P_1^{\text{nc}}$ , [2], the Bernardi–Raugel space, [1] and the modified Crouzeix–Raviart space, [13]. The non-conforming Crouzeix–Raviart space and the Bernardi–Raugel space can be applied also on tetrahedral grids. On quadrilateral and hexahedral grids one can use the rotated bilinear finite element space  $Q_1^{\text{rot}}$ , [15]. For all these spaces, the  $H^1$ -semi norm on the right hand side of (8) has to be replaced by a discrete  $H^1$ -semi norm which is computed mesh cell by mesh cell. The majority of finite element codes does not provide finite element spaces which are subspaces of  $H^2(\Omega)$  such that a higher regularity of  $p_{\text{sep}}$  than  $H^1(\Omega)$  cannot be achieved using such codes. Thus, the case  $k = 1$  is the most important one and we will restrict our numerical studies to this case.

### 3. The studied variants for computing a separated pressure $p_{\text{sep}}$

In this paper, we will assess five different techniques for computing  $p_{\text{sep}}$  which will be presented in this section.

#### 3.1. Variant 1

The application of the pressure separation requires a good approximation of  $p$ . In the first variant, we will use the approximation of  $p$  which is computed by solving the Navier–Stokes equations (1), namely the finite element solution  $p^h$ . Since  $p^h$  is piecewise constant, it is not in  $H^1(\Omega)$ . Therefore we cannot directly use  $p^h$  as separated pressure. Instead, we use an interpolation  $I_1(p^h)$  of  $p^h$  into the first order finite element space consisting of continuous functions  $P_1(Q_1)$ . This interpolation is based on local averaging, see [19,11,8] for details of the averaging operator and its implementation. Thus, Variant 1 of the pressure separation looks as follows:

- Compute the finite element solution  $(\mathbf{u}^h, p^h)$  for the original Navier–Stokes equations (1).
- Compute  $p_{\text{sep}} = I_1(p^h)$ .
- Compute the finite element solution  $(\mathbf{u}_{\text{sep}}^h, p_{\text{sep}}^h)$  of the pressure-separated Navier–Stokes equations (9).
- Assign  $\mathbf{u}_{\text{NSE}}^h = \mathbf{u}_{\text{sep}}^h$ ,  $p_{\text{NSE}}^h = p^h + p_{\text{sep}}^h$ .

#### 3.2. Variant 2

Variant 1 has the disadvantage that it requires the solution of the Navier–Stokes equations two times. Thus, one can expect that it needs roughly twice the computing time of solving the Navier–Stokes equations without pressure separation. The numerical tests will confirm this expectation, see Section 4.3. One idea to improve this aspect is to solve the original Navier–Stokes equations (1) only approximately using a small fixed number of iterations or a weak stopping criterion. From the many possibilities in this approach, we tested this one, that only one step in the fixed point iteration of the Navier–Stokes equations is applied. As initial guess  $(\mathbf{u}^{h,0}, p^{h,0})$ , the interpolation of the solution from the previous level is used. After the first iteration step, one obtains  $(\mathbf{u}^{h,1}, p^{h,1})$  and we set  $p_{\text{sep}} = I_1(p^{h,1})$ . The other steps of this variant are the same as of Variant 1.

#### 3.3. Variant 3

The third approach is motivated by the fact that the pressure separation should improve the computational results for higher Reynolds number  $Re$ .

Neglecting for higher  $Re$  the viscous term in the Navier–Stokes equations (1) and also the non-linear convective term gives the equation  $\nabla p = \mathbf{f}$ . Applying the divergence operator to this equation and equipping it with homogeneous Neumann boundary condition gives an equation to compute a separated pressure  $p_{\text{sep}} \in H^1(\Omega) \cap L_0^2(\Omega)$

$$\begin{aligned} -\Delta p_{\text{sep}} &= -\nabla \cdot \mathbf{f} \quad \text{in } \Omega, \\ \frac{\partial p_{\text{sep}}}{\partial \mathbf{n}} &= 0 \quad \text{on } \partial\Omega, \\ \int_{\Omega} p_{\text{sep}} \, d\mathbf{x} &= 0. \end{aligned} \tag{10}$$

The use of homogeneous Neumann boundary condition was proposed in [3]. Problem (10) will be discretised by first order conforming finite elements  $P_1(Q_1)$ . This is in contrast to [3], where (10) was discretised with non-conforming finite elements of lowest order ( $P_1^{\text{nc}}$ ). The arising scalar discrete equation is solved very effectively by using a multigrid method.

### 3.4. Variants 4 and 5

Variants 4 and 5 are extensions of Variant 3. Let  $\mathbf{u}_0^h$  be an approximation of  $\mathbf{u}$ . Then the non-linear convective term is not simply neglected in the equation for  $p_{\text{sep}}$  as in Variant 3 but it is put on the right hand side of the equation for  $p_{\text{sep}}$ . Thus one has to solve

$$\begin{aligned} -\Delta p_{\text{sep}} &= -\nabla \cdot (\mathbf{f} - (\mathbf{u}_0^h \cdot \nabla) \mathbf{u}_0^h) \quad \text{in } \Omega, \\ \frac{\partial p_{\text{sep}}}{\partial \mathbf{n}} &= 0 \quad \text{on } \partial\Omega, \\ \int_{\Omega} p_{\text{sep}} \, d\mathbf{x} &= 0. \end{aligned} \tag{11}$$

There are of course many possibilities to obtain an approximation  $\mathbf{u}_0^h$ , e.g., taking the interpolation of the solution from the previous level or solving the original Navier–Stokes equations on the given level approximately (like in Variant 2) or solving them even accurately (like in Variant 1). Variant 4 is the simplest of these possibilities, namely to take the interpolation of the solution from the previous level. In Variant 5, we used for  $\mathbf{u}_0^h$  the iterate which is computed with the first step of the non-linear iteration (this is  $\mathbf{u}^{h,1}$  in Variant 2). An interpolation of the non-conforming discrete velocity  $\mathbf{u}_0^h$  into a conforming finite element space was not applied since the term  $(\mathbf{u}_0^h \cdot \nabla) \mathbf{u}_0^h$  is needed in the assembling of the right hand side of (11) only in quadrature points in the interior of mesh cells.

In many applications there is  $\mathbf{f} = \mathbf{0}$ . Thus, whereas in this case one can compute a separated pressure  $p_{\text{sep}}$  with Variants 4 and 5, one obtains only the trivial solution with Variant 3.

#### 4. The numerical studies

The numerical tests will study the following two questions for the variants of computing a separated pressure which were presented in previous section:

- Does the error in the discrete velocity becomes smaller if the pressure-separated Navier–Stokes equations (9) are solved instead of the original Navier–Stokes equations (1)?
- How much is the overhead for computing an appropriate separated pressure  $p_{\text{sep}}$  and solving (9)?

The numerical studies involve two-dimensional as well as three-dimensional examples. They were performed using the non-conforming bilinear rotated finite element discretisation  $Q_1^{\text{rot}}/Q_0$  and the Crouzeix–Raviart finite element  $P_1^{\text{nc}}/P_0$ . The computations were carried out with the code MooNMD [8,11].

In all figures, ‘Var. 0’ stands for solving the Navier–Stokes equations (1) without pressure separation.

##### 4.1. Two-dimensional tests

For the two-dimensional tests, we have chosen  $\Omega = (0, 1)^2$ ,  $Re = 1000$  and the prescribed velocity field  $\mathbf{u} = (u_1, u_2)$  and the pressure  $p$  where

$$\begin{aligned} u_1 &= 2x^2(1-x)^2(y(1-y)^2 - y^2(1-y)), \\ u_2 &= -2y^2(1-y)^2(x(1-x)^2 - x^2(1-x)), \\ p &= x^3 + y^3 - 0.5. \end{aligned} \tag{12}$$

The velocity fulfills homogeneous Dirichlet boundary conditions. The right hand side  $\mathbf{f}$  was chosen such that  $(\mathbf{u}, p)$  fulfill the Navier–Stokes equations (1) for the given Reynolds number.

Computations were performed on triangular grids with the  $P_1^{\text{nc}}/P_0$  finite element and on rectangular grids with the  $Q_1^{\text{rot}}/Q_0$  finite element. The initial triangular grid (level 0) is shown in Fig. 1. On this unstructured grid, any superconvergence effects can be excluded. The initial rectangular grid consists of four squares with edge length 0.5. The grids were refined uniformly. On the finest level 9, there are 9,439,744 degrees of freedom on the triangular grid and 5,246,976 degrees of freedom on the rectangular grid.

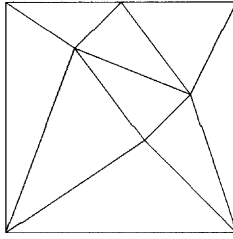


Fig. 1. Coarse grid for the computations with  $P_1^{nc}/P_0$  in 2d.

The numerical results for the velocity errors in the  $L^2$ -norm and the  $H^1$ -semi norm are presented in Fig. 2. The results for the  $P_1^{nc}/P_0$  and the  $Q_1^{rot}/Q_0$  finite element are very similar. With all variants of the pressure separation, the computed solutions are more accurate than without pressure separation. Using Variants 1 and 2, which are based on approximations of the discrete pressure computed without pressure separation, the gain in the error is roughly one order of magnitude. The differences between Variants 1 and 2 are rather small.

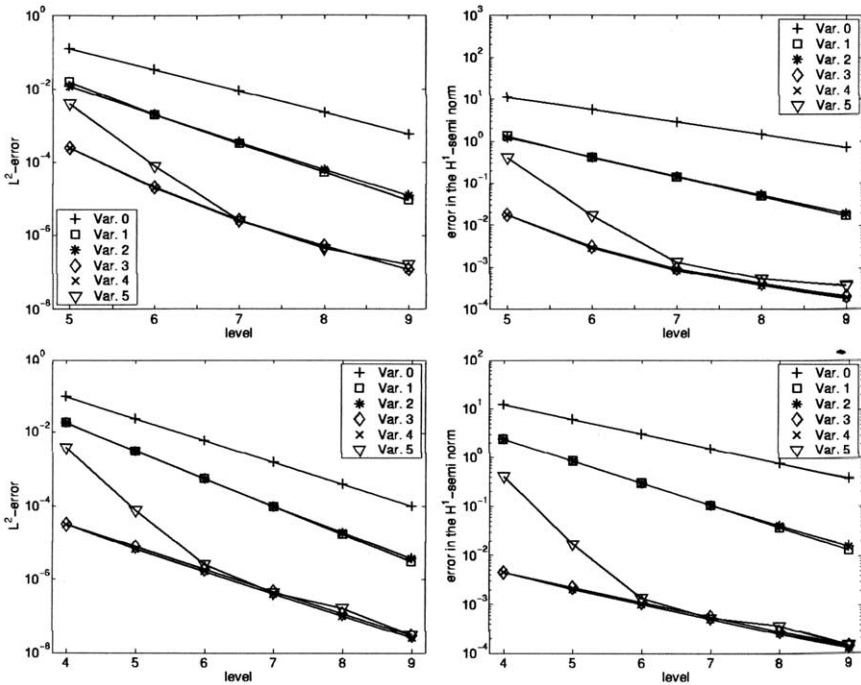


Fig. 2. 2d example, velocity errors, left  $L^2$ -norm, right  $H^1$ -semi norm, top  $P_1^{nc}/P_0$ , bottom  $Q_1^{rot}/Q_0$ .

With Variants 3 and 4, which are based on the solution of an auxiliary problem, the gain in the errors is three to four orders of magnitude. Only very small differences can be observed between these variants. The results for Variant 5 are in between the other variants. On coarse grids, the gain in the error is better than with Variants 1 and 2 but worse than with Variants 3 and 4. On fine grids, Variant 5 behaves similar to Variants 3 and 4.

Computational studies were performed also with lower Reynolds numbers than 1000. The qualitative results of these studies are the same as with  $Re = 1000$ , namely, the application of all variants of pressure separation resulted in numerical solutions with smaller errors. However, quantitatively, we observed that the gain in the error reduction was smaller for smaller Reynolds numbers, compare also the three-dimensional tests. This effect can be expected since the pressure separation is a technique which is proposed for higher Reynolds numbers, see Section 2.

#### 4.2. Three-dimensional tests

The three-dimensional tests were performed on the unit cube  $\Omega = (0, 1)^3$  with the prescribed velocity  $\mathbf{u} = (u_1, u_2, u_3)$  and pressure  $p$

$$\begin{aligned} u_1(x, y, z) &= \alpha(\sin(\pi x) \sin(\pi y) \sin(\pi z) + x^4 \cos(\pi y)), \\ u_2(x, y, z) &= \alpha(\cos(\pi x) \cos(\pi y) \cos(\pi z) - 3y^3 z), \\ u_3(x, y, z) &= \alpha(\cos(\pi x) \sin(\pi y) \cos(\pi z) + \cos(\pi x) \sin(\pi y) \sin(\pi z) \\ &\quad - 4x^3 z \cos(\pi y) + 4.5y^2 z^2), \\ p(x, y, z) &= 3x - \sin(y + 4z) + c. \end{aligned}$$

The constant  $c$  was chosen such that  $p \in L_0^2(\Omega)$ . With the parameter  $\alpha \in \mathbb{R}$  it is possible to consider flows which are dominated by the pressure gradient ( $\alpha$  close to zero) and also flows which are dominated by the velocity (absolute value of  $\alpha$  large). From the motivation of the pressure separation and also from the error estimate (8) for the Stokes equations, it becomes clear that a positive effect of applying a pressure separation can be expected in particular for flows which are dominated by the pressure gradient.

We will present computations for the  $P_1^{\text{nc}}/P_0$  finite element on tetrahedral grids and the  $Q_1^{\text{rot}}/Q_0$  finite element on hexahedral grids. The Reynolds numbers for which the solution of the stationary Navier–Stokes equations in 3d was possible are much smaller than the Reynolds numbers for which these equations can be solved in 2d. Thus, we will present results with  $Re = 30$  for the  $P_1^{\text{nc}}/P_0$  finite element discretisation and with  $Re = 50$  for the  $Q_1^{\text{rot}}/Q_0$  finite element discretisation. The right hand side and the boundary conditions of the Navier–Stokes equations (1) were chosen such that  $(\mathbf{u}, p, Re)$  satisfies these equations.

The initial tetrahedral grid (level 0) consist of six tetrahedra and the initial hexahedral grid of eight cubes of side length 0.5. On the finest level, there are 11,083,776 degrees of freedom on the tetrahedral grid (level 6) and 2,658,304 degrees of freedom on the hexahedral grid (level 5).

The computational results are presented in Figs. 3 and 4. We will first discuss the results for the pressure gradient dominated flows, i.e.,  $\alpha = 0.25$  for the  $P_1^{nc}/P_0$  finite element and  $\alpha = 0$  for the  $Q_1^{rot}/Q_0$  finite element. These results are qualitatively similar to the results of the 2d computations. All variants of the pressure separation lead to a decrease in the errors. The results obtained with Variants 3 and 4 are again in general more accurate than with Variants 1 and 2. On the hexahedral grid,  $Q_1^{rot}/Q_0$  with  $\alpha = 0$ , Variant 5 behaves like in the 2d tests. On the tetrahedral grid,  $P_1^{nc}/P_0$  with  $\alpha = 0.25$ , Variant 5 gives almost identical results as Variant 4. The gain in the error is about one order of magnitude for  $P_1^{nc}/P_0$ ,  $\alpha = 0.25$ , and up to four orders of magnitude for  $Q_1^{rot}/Q_0$ ,  $\alpha = 0$ . Altogether, the application of the pressure separation leads to a considerable improvement of the discrete velocity for pressure gradient dominated flows.

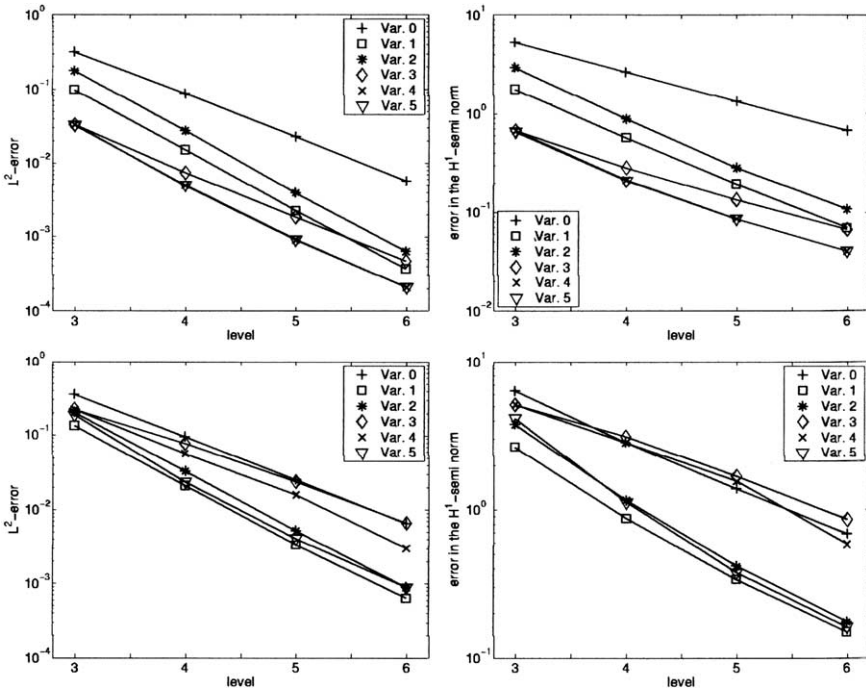


Fig. 3. 3d example, velocity errors, left  $L^2$ -norm, right  $H^1$ -semi norm,  $P_1^{nc}/P_0$ , top  $\alpha = 0.25$ , bottom  $\alpha = 1$ .

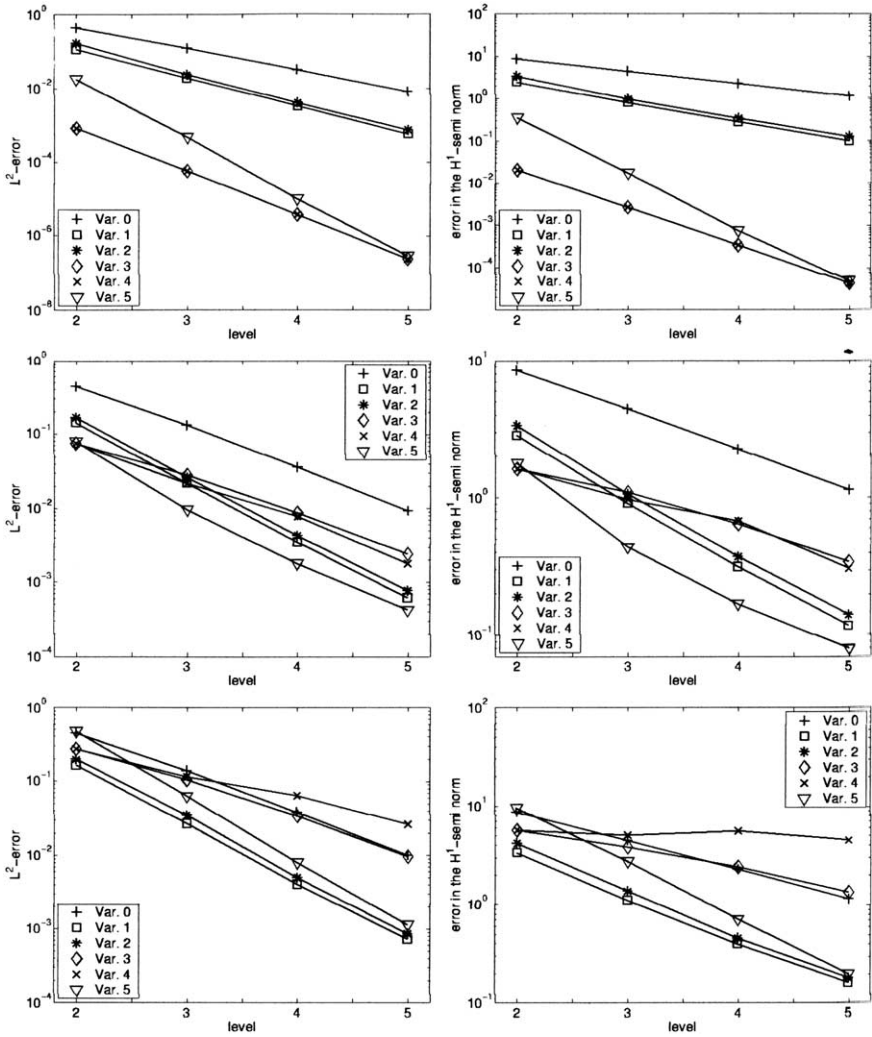


Fig. 4. 3d example, velocity errors, left  $L^2$ -norm, right  $H^1$ -semi norm,  $Q_1^{\text{rot}}/Q_0$ , top  $\alpha = 0$ , middle  $\alpha = 0.5$ , bottom  $\alpha = 1$ .

If the flow becomes more velocity dominated ( $\alpha = 0.5$  and 1), the situation changes somewhat. Applying Variants 1 and 2 of the pressure separation gives still a decrease of the error (0.5–1 order of magnitude). In contrast, the errors of the solutions computed with Variants 3 and 4 are sometimes larger than the errors of the solution without pressure separation. Using a better velocity approximation in the auxiliary problem, i.e., Variant 5 instead of Variant 4,

leads to a considerable improvement of the results. In summary, using a pressure separation has less effect for velocity dominated flows. But for some variants of the pressure separation, there is still a notable gain of accuracy.

#### 4.3. Computational overhead and assessment of the variants for computing a separated pressure

The application of the pressure separation requires additional computational efforts. These are the computation of an approximation of  $p^h$  (Variants 1 and 2) and the solution of an auxiliary problem (Variants 3–5). In this section, first the additional overhead in terms of computing time is assessed. The discrete Navier–Stokes equations are solved by a preconditioned flexible GMRES method, [16]. As preconditioner, the multiple discretisation multilevel method is applied, see Section 1 for a short explanation or [7,8] for details of this method. This approach has been proven to be efficient and robust in a numerical study for solving the stationary 3d Navier–Stokes equations governing the flow around a cylinder, [7]. In our computations, this solver was applied with the same parameters in all tests.

For assessing the computational overhead, we took the solution time for the Navier–Stokes equations without pressure separation as unit (100%) for each example. The relative computing times to this unit are presented in Table 1. As expected in Section 3, the application of Variant 1 roughly doubles the computing time. In contrast, the computational overhead for Variant 2 is in general only about 10% or below. Since the error reduction is very similar for both of these variants, Variant 2 has to be preferred for the reason of less computational overhead. The computational overhead for Variants 3–5 is larger than for Variant 2, but in general considerably smaller than for Variant 1. There are small differences among Variants 3–5 in the computational overhead for the 2d computations and the pressure gradient dominated 3d computations. For the velocity dominated 3d computations, Variant 5 has the smallest

Table 1

Relative computing times compared to the computing time for solving the Navier–Stokes equations without pressure separation (100%)

Example	Var. 0	Var. 1	Var. 2	Var. 3	Var. 4	Var. 5
2d, $P_1^{\text{nc}}/P_0$	100	198	103	108	111	98
2d, $Q_1^{\text{rot}}/Q_0$	100	174	97	110	111	106
3d, $P_1^{\text{nc}}/P_0, \alpha = 0.25$	100	249	158	142	142	157
3d, $P_1^{\text{nc}}/P_0, \alpha = 1$	100	192	112	146	146	112
3d, $Q_1^{\text{rot}}/Q_0, \alpha = 0$	100	187	110	122	124	138
3d, $Q_1^{\text{rot}}/Q_0, \alpha = 0.5$	100	184	103	159	161	132
3d, $Q_1^{\text{rot}}/Q_0, \alpha = 1$	100	187	96	191	160	110

overhead. Altogether, based on the computational overhead, no ranking of the Variants 3–5 can be done.

Considering the error reductions obtained with Variants 2–5, one finds that in 2d and the pressure gradient dominated 3d computations, Variants 3 and 4 are best and Variant 2 is by far worst. Variant 5 is, at least for finer levels, close to Variants 3 and 4. In the velocity dominated 3d computations, Variants 3 and 4 are worse than Variants 2 and 5. If the nature of the flow is known a priori, these results give an indication which variant should be used. In the case that the nature of the flow is unknown, we recommend to use Variant 5 since the results obtained with this variant were on finer levels in all case close to the best ones.

#### 4.4. Some possible extensions

We think that a more sophisticated modification of Variant 5, e.g., by solving first the Navier–Stokes equations up to a certain accuracy before solving the auxiliary problem to compute  $p_{\text{sep}}$ , will improve the results further.

Another approach, which was proposed in [18], consists in solving an auxiliary problem of form (11) in each step of the non-linear iteration for solving the Navier–Stokes equations. The function  $\mathbf{u}_0^h$  in (11) is the current iterate of the discrete velocity.

The pressure separation can be applied also to the time-dependent Navier–Stokes equations, e.g., see [6]. For these equations, there is an easy way for choosing  $p_{\text{sep}}$ , namely by taking the discrete pressure solution from the previous discrete time. In particular, in the case of small time steps, there will be in general only a small difference in the pressures of two consecutive discrete times. Thus, the discrete pressure from the previous discrete time will be a good approximation of the pressure in the current discrete time.

## 5. Summary

The paper presented numerical studies of applying the pressure separation, which is a technique to improve the accuracy of the discrete velocity in finite element solutions of the Navier–Stokes equations in the case of higher Reynolds numbers. It turned out that this technique can be applied above all for lowest order non-conforming finite element discretisations of the Navier–Stokes equations. Five different variants of computing a separated pressure were compared at two- and three-dimensional examples. The application of the pressure separation led in the most cases to a considerable decrease of the velocity errors. This decrease was large especially for pressure gradient dominated flows. Based on the error decrease and the computational overhead, none of the studied variants to compute a separated pressure can be clearly preferred. However, a good choice in all cases was Variant 5.

## Acknowledgement

The work of S. Ganesan has been supported by the Deutsche Forschungsgemeinschaft (DFG) within the graduate program, *Micro-Macro-Interactions in Structured Media and Particle Systems*.

## References

- [1] C. Bernardi, G. Raugel, Analysis of some finite elements for the Stokes problem, *Math. Comp.* 44 (1985) 71–79.
- [2] M. Crouzeix, P.-A. Raviart, Conforming and nonconforming finite element methods for solving the stationary Stokes equations I, *R.A.I.R.O. Anal. Numér.* 7 (1973) 33–76.
- [3] O. Dorok, Improved accuracy of a finite element discretization for solving the Boussinesq approximation of the Navier–Stokes equations, Preprint 32/94, Otto-von-Guericke-Universität Magdeburg, Fakultät für Mathematik, 1994.
- [4] V. Girault, P.-A. Raviart, *Finite Element Methods for Navier–Stokes Equations*, Springer-Verlag, Berlin, Heidelberg, New York, 1986.
- [5] P.M. Gresho, R.L. Sani, *Incompressible Flow and the Finite Element Method*, Wiley, Chichester, 2000.
- [6] V. John, Parallele Lösung der inkompressiblen Navier–Stokes Gleichungen auf adaptiv verfeinerten Gittern. PhD thesis, Otto-von-Guericke-Universität Magdeburg, Fakultät für Mathematik, 1997.
- [7] V. John, Higher order finite element methods and multigrid solvers in a benchmark problem for the 3D Navier–Stokes equations, *Int. J. Num. Meth. Fluids* 40 (2002) 775–798.
- [8] V. John, Large Eddy Simulation of Turbulent Incompressible Flows. Analytical and Numerical Results for a Class of LES Models, *Lecture Notes in Computational Science and Engineering*, vol. 34, Springer-Verlag Berlin, Heidelberg, New York, 2003.
- [9] V. John, P. Knobloch, G. Matthies, L. Tobiska, Non-nested multi-level solvers for finite element discretizations of mixed problems, *Computing* 68 (2002) 313–341.
- [10] V. John, G. Matthies, Higher order finite element discretizations in a benchmark problem for incompressible flows, *Int. J. Num. Meth. Fluids* 37 (2001) 885–903.
- [11] V. John, G. Matthies, MooNMD—a program package based on mapped finite element methods, *Comput. Visual. Sci.* 6 (2004) 163–170.
- [12] V. John, L. Tobiska, Smoothers in coupled multigrid methods for the parallel solution of the incompressible Navier–Stokes equations, *Int. J. Num. Meth. Fluids* 33 (2000) 453–473.
- [13] P. Knobloch, On the application of the  $P_1^{\text{mod}}$  element to incompressible flow problems, *Comput. Visual. Sci.* 6 (2004) 185–195.
- [14] G. Matthies, P. Skrzypacz, L. Tobiska, Superconvergence of a 3d finite element method for stationary Stokes and Navier–Stokes problems, Preprint 19, Fakultät für Mathematik, Otto-von-Guericke-Universität Magdeburg, 2003.
- [15] R. Rannacher, S. Turek, Simple nonconforming quadrilateral Stokes element, *Numer. Meth. Part. Diff. Eq.* 8 (1992) 97–111.
- [16] Y. Saad, A flexible inner–outer preconditioned GMRES algorithm, *SIAM J. Sci. Comput.* 14 (2) (1993) 461–469.
- [17] M. Schäfer, S. Turek, The benchmark problem “Flow around a cylinder”, in: E.H. Hirschel, (Ed.), *Flow Simulation with High-Performance Computers II*, Notes on Numerical Fluid Mechanics, vol. 52, Vieweg, 1996, pp. 547–566.

- [18] F. Schieweck, Parallele Lösung der stationären inkompressiblen Navier–Stokes Gleichungen, Otto-von-Guericke-Universität Magdeburg, Fakultät für Mathematik, 1997, Habilitation.
- [19] F. Schieweck, A general transfer operator for arbitrary finite element spaces, Preprint 00-25, Fakultät für Mathematik, Otto-von-Guericke-Universität Magdeburg, 2000.
- [20] S. Turek, Efficient solvers for incompressible flow problems: an algorithmic and computational approach, Lecture Notes in Computational Science and Engineering, vol. 6, Springer, 1999.